Materials Research Proceedings 41 (2024) 224-233 https://doi.org/10.21741/9781644903131-25

Numerical modeling of the compressive behavior of 316L body-centered cubic lattice structures

RÍOS Ignacio[1,2,a], MARTÍNEZ Alex[1,b], SAGGIONETTO Enrico[3,c], MERTENS Anne[3,d], DUCHÊNE Laurent[4,e], HABRAKEN Anne Marie[4,f], TUNINETTI Víctor[1,*,g]

[1]Department of Mechanical Engineering, Universidad de La Frontera, Temuco, Chile

[2]Master in Engineering Sciences, Universidad de La Frontera, Temuco, Chile

[3]Department A&M-MMS, University of Liège, Liège, Belgium

[4]Department ArGEnCo-MSM, University of Liège, Liège, Belgium

[a]ignacio.rios@ufrontera.cl, [b]a.martinez16@ufromail.cl, [c]enrico.saggionetto@uliege.be, [d]anne.mertens@uliege.be, [e]l.duchene@uliege.be, [f]anne.habraken@uliege.be, [g]victor.tuninetti@ufrontera.cl

Keywords: Lattice Structure, Additive Manufacturing, Relative Density

Abstract. With additive manufacturing, innovative porous structures emerge for generating lightweight components with high mechanical responses. Body-centered cubic lattice structures are the focus of this study, with customizable lattice density depending on the strut diameter. To predict the properties of lattice structures and thus reduce the number of tests in experimental campaigns, several numerical and analytical models have been developed. In this work, the elastoplastic response was determined. Buckling phenomena of vertical struts depend on the different boundary conditions applied in Finite Element simulations. As shown the number of cells within the model affects the results. This size effect was quantified for different lattice density cases. The numerical results obtained for lattice structures with different relative density were also compared with the well-known Gibson-Ashby model.

Introduction

The development of additive manufacturing technologies and their fabrication capacities has enabled the production of parts with complex three dimensional geometries. These capabilities allow producing parts with innovative designs [1], optimized functionalities [2] and lightweight structures [3] while reducing production cost. Indeed, this process decreases material consumption, production time and post-processing. The lattice structures belong to the complex components built by additive manufacturing.

Lattice structures are based on a cellular representative unit, which is repeated in an orderly fashion in a three-dimensional space. The basic cells – generally called struts-based cells – are defined by constituent rods, with particular geometric dimensions and connectivity at certain points in space called nodes, thus defining their topology. From a cellular point of view, lattice structures can be considered indeed as local structures [4], but from a more macroscopic point of view, they can be considered as a homogenized meta-material distributed in a three-dimensional space with its own mechanical properties [5].

One of the main features of lattice structures is that their global mechanical response can be altered by modifying their topology or geometry parameters such as relative density, cell topology, cell size, among other design parameters. Depending on its design, the lattice structure leads to mechanical properties that significantly differ from those of the constituent material [6].

Content from this work may be used under the terms of the Creative Commons Attribution 3.0 license. Any further distribution of this work must maintain attribution to the author(s) and the title of the work, journal citation and DOI. Published under license by Materials Research Forum LLC.

Cellular structures have been used in several applications, such as aerospace [7], automotive [8], marine [9] and medical [10] industries, owing to the lightweight nature, high strength-to-weight ratio, potential for customization and specific energy absorption capacity [11, 12].

On the basis of the mechanical response, lattice structures can be categorized into bending-dominated or stretch-dominated. Bending-dominated lattice structures experience mostly internal bending moments and are therefore compliant, while stretch-dominated lattice structures experience mainly internal axial loads and are therefore stiffer than bending-dominated structures. In general, the cell topology is the main factor that defines the deformation mechanism of the lattice structure [13].

The most studied strut-based lattice structure topologies are those based on body-centered cubic (BCC), face-centered cubic (FCC) geometries and their variants with reinforcing struts, with the most common one being z reinforcement in the direction of the load (BCCZ and FCCZ). The behavior of these strut-based cells can be characterized by the connectivity of the struts defined in Eq. 1 with the Maxwell number [5, 14], (M). This M-value depends on the number of struts (s) of the representative cell, and the number of nodes, (n).

$$M = s - 3n + 6 \tag{1}$$

For $M < 0$, the system is bending-dominated, while for $M \geq 0$ the structure will display a stretch-dominated behavior. This number is just a general indicator, as the boundary between the two types of behavior is not so clear. It also depends on the orientation of struts versus the load direction.

To decrease the experimental campaigns, many computational models, based on the finite element method, have been developed with the goal of predicting the mechanical behavior of lattice structures, especially those related with the energy absorption capacity of such structures. For instance, Rodrigo et al. [15] presented the quasi-static and dynamic compression behavior of functionally graded lattices by means of experiments and simulations using finite element modeling. The successful validation of their model allowed parametric simulations of the structure subjected to higher compression rates. Wang et al. [13] also investigated the mechanical response and deformation mechanism of a hierarchical lattice structure by means of quasi-static compression tests and numerical simulations. They also found out a good correlation between both methods and proved a superior performance of strut-reinforced hierarchical lattice structures compared to conventional ones. Favre et al. [6] used a continuous crystallographic approach to generate cubic strut-based lattice cells with different topologies and evaluated them through finite element modeling. They found a relationship between the relative elastic modulus and relative density equivalent to the Gibson-Ashby model, with a constant $C = 1$ and an exponent n dependent on the cell topology and geometry.

Computational models have proven to be reliable tools to predict the mechanical behavior of lattice structures, validating analytical models such as the Gibson-Ashby model [16]. However, there is a lack of models evaluating the effect of different boundary conditions in simulations compared with real physical experiments. The present article assesses the impact of the size effect, in terms of number of cells in the studied volume, on the global elastoplastic response of a body centered cubic lattice. The simulations are performed with various boundary conditions and relative densities. They demonstrate the great importance of taking into account the edge effect in lattice structures. Indeed different numbers of cells generate different mechanical responses. The insights and findings reported in this work must be considered when modeling lattice structures as a homogenized material in small domains.

Materials Research Proceedings 41 (2024) 224-233 https://doi.org/10.21741/9781644903131-25

Materials and Methods

Strut-based lattice structure

The investigated body-centered cubic lattice cells with strut reinforcements on the x, y and z axes (BCCXYZ lattice) at different relative densities are shown in Fig. 1. Four BCCXYZ cells with different relative densities of 20%, 40%, 60% and 80% were modeled by adapting the diameter of the representative strut. The cell size L was set constant at a value of 3 mm. The parameters for defining the topology of the cells shown in Fig.1 are the relative density (ρ_r), the strut diameter (d) and the cell size (L).

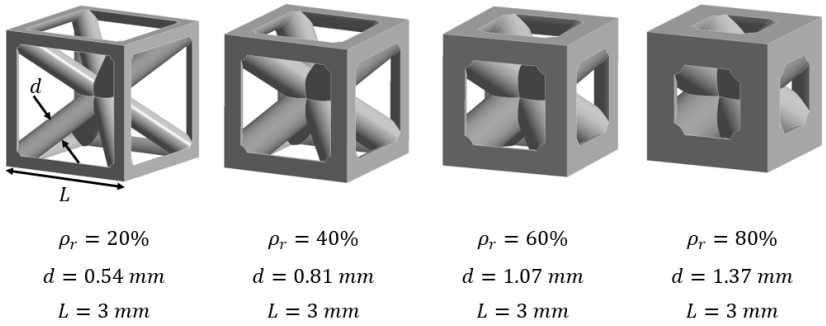

Fig. 1 Lattice cell designs at different relative densities $\boldsymbol{\rho_r}$ and their geometric parameters: strut diameter $\boldsymbol{d}$ and cell size $\boldsymbol{L}$.

Finite element modeling

Finite element models of the four lattice structures shown in Fig. 1 were designed with their different relative density using ANSYS mechanical. To reveal the different mechanical responses of these structures under different boundary conditions, four models (see Fig. 2) were implemented:

- Model 1 is made up of a single cell without any displacement constraints applied to the lateral faces. In the bottom face, the degree of freedom in the Y direction (direction perpendicular to the face) is constrained, allowing lateral displacements within this face. A reference line in the center of the cell was defined having only its degree of freedom of displacement in the Y direction free. It aims to prevent any side slip or rigid movement of the whole sample. A constant displacement of 0.3 mm was applied to all the nodes in the upper face of the cell to apply an overall compression strain up to 10%.
- Model 2 is made up of a single cell with three symmetry planes in faces which are respectively perpendicular to each of the three x, y and z coordinate axes. By this way, a structure of eight cells is represented. A constant displacement of 0.6 mm was applied to all the nodes in the upper face of the cell.
- Model 3 is made up of a single cell with three symmetry planes perpendicular to each of the three x, y and z coordinate axes. Additionally, on the two remaining lateral faces, the constraint that all the nodes of these faces should remain in the same plane is applied. In other words, these lateral faces are allowed to move as long as they stay flat, preventing buckling or any similar effect. A constant displacement of 0.6 mm was applied to all the nodes in the upper face of the cell.
- Model 4 is made up of 8 cells with three symmetry planes in faces perpendicular to each of the three x, y and z coordinate axes. In this way, a structure of 64 cells is represented. A constant displacement of 1.2 mm was applied to all the nodes in the upper face of the model.

For all the simulations, an overall compression strain up to 10% was applied.

The struts of the lattice structures were meshed using solid elements SOLID187 of size between 0.13 and 0.2 mm. The material properties were set based on the 316L stainless steel. A bilinear elastic-plastic model was chosen considering the 316L strain-hardening after the yield point. The elastic modulus was set to 150 GPa, the yield stress to 225 MPa and the hardening modulus to 0.95 GPa. Poisson's ratio was established as 0.3.

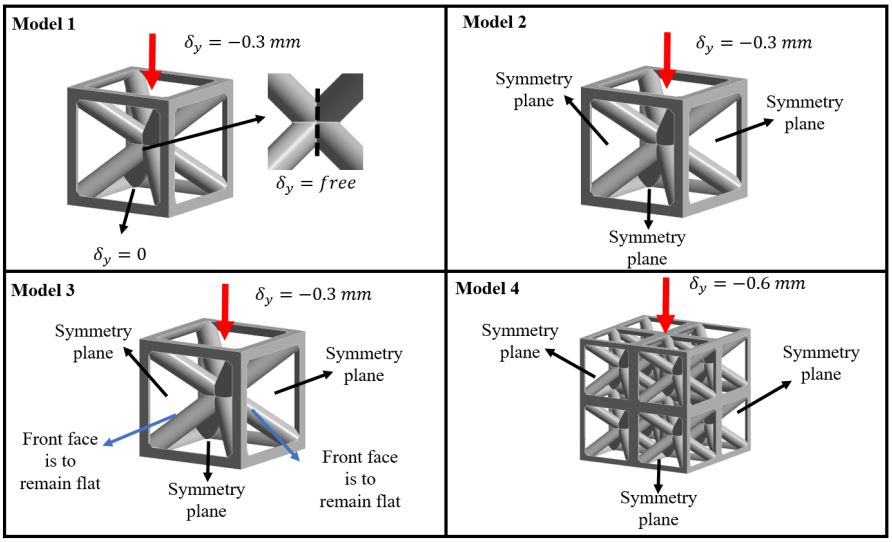

Fig. 2 Graphical representation of the four models with different boundary conditions applied on a 20% relative density lattice cell.

Methodology to assess lattice mechanical properties

The mechanical properties of lattice structures have a slightly different interpretation with respect to the standard definitions of solid materials. For example, elastic modulus, yield strength and tangent modulus, when determined for lattice structures, refer to the apparent macroscopic properties that converge to certain values when the number of unit cells is sufficiently large [17].

Usually the mechanical properties of lattice structures are expressed as a fraction of the corresponding mechanical property of the solid material. This ratio depends on the relative density of the cellular unit. Density fraction (ρ/ρ_0) is defined as the ratio between the density of the lattice structure (ρ) and the density of the bulk material from which it is built (ρ_0) [17]. In general, and regardless of their topology, the mechanical properties of lattice structures tend to increase with an increment in their relative density. Another factor that plays a relevant role regarding the mechanical response of anisotropic lattice structures is the orientation of the cells with respect to the loading direction.

Most mechanical characterizations of lattice structures are performed through compression tests, due to their simple performance in contrast with tensile tests. The problem in the tensile case is linked to the design of a specimen that avoids stress concentration [18]. The compressive deformation mechanism of lattice structures can be divided into three stages: a linear elastic deformation, followed by plastic deformation and ending in densification or compaction (Fig. 3) [19]. Within the compression test, the individual struts of the lattice structures are prone to failure by 3 mechanisms: yielding, buckling and fracture [5].

During the elastic deformation stage, the stress-strain response of the cellular material is linear elastic, with an elastic modulus proportional to the elastic modulus of the parent material. Once the elastic limit is reached, plastic deformation takes place and yielding or buckling begins in the cells of the lattice structure. Often plastic deformation continues with an almost constant stress, known as plateau stress [5]. Additionally, at this stage, it is possible to experience an oscillating stress behavior, due to the consecutive failure of the different cell layers of the lattice structure.

This effect is further enhanced due to the inherent fabrication defects of additive manufacturing. Once the deformations of the cells are high enough to present contact between the different layers of the lattice material, the densification or compaction stage is reached. At this stage, the stress necessary to increase the deformation abruptly grows and the cellular material adopts a behavior closer to that of the solid material (see Fig. 3).

From the macroscopic point of view of cellular material, three main modes of compressive failure have been found: i) successive collapse of cells, in which each layer collapses due to buckling or crushing, and compresses on the layer below, making the structure stronger after the compaction of each layer; ii) brittle fracture in the cell walls, usually originated by the existence of some defects and characterized by the propagation of the crack or cracks through the lattice struts; and iii) diagonal shear, resulting in an initial loss of about 50% of strength followed by a stiffening during densification [20].

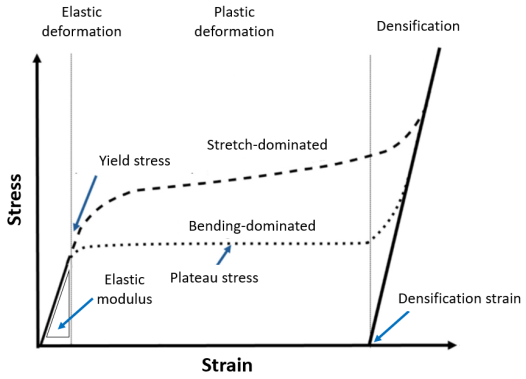

Fig. 3 Stress-strain compression curves characteristic of bending-dominated and stretch-dominated lattice structures. Modified from [19]

The Gibson-Ashby model is one of the most widely accepted models for computing the mechanical properties of cellular structures including strut-based lattice structures. This model predicts mechanical properties, such as elastic modulus and yield strength, expressed as fractions of the base material properties. These properties depend on the type of mechanical response of the lattice structure, whether bending-dominant or stretch-dominant. They are expressed as a positive power relation with the relative density of the lattice structure. The formulation for the elastic modulus and yield strength for lattice structures is shown in Eq. 2 and Eq. 3, respectively [16]:

$$\frac{E}{E_0} = C\left(\frac{\rho}{\rho_0}\right)^n \tag{2}$$

$$\frac{\sigma}{\sigma_0} = C\left(\frac{\rho}{\rho_0}\right)^n \tag{3}$$

where E and σ are the apparent elastic modulus and yield strength of the lattice structure, E_0 and σ_0 are the elastic modulus and yield strength of the bulk parent material. Following this way, the fractions (E/E_0) and (σ/σ_0) can be defined as the relative modulus and the relative strength of the lattice structure, with C being the Gibson-Ashby constant. Its value depends on the cell topology and geometry and should be derived from experimental results. The exponent n depends on the mechanical response of the lattice structure, bending or stretch-dominated. It has different values depending on cell geometry size and materials. However, this exponent value is also usually derived from experimental results.

In this work, the presented model with different relative densities, numbers of cells and boundary conditions were simulated up to a global strain of 10%. The global stress-strain curves

were calculated and used to derive the Gibson-Ashby exponent n, assuming a constant C value of 1. The procedure was applied on the modulus of elasticity, the tangent modulus and the yield stress (defined for 0.2% of plastic strain).

Results

Figure 4 shows the global true stress-strain curves of simulated BCCXYZ lattice structure with 5 different relative densities and the boundary condition expressed in model 2, thus representing an 8 cell lattice structure.

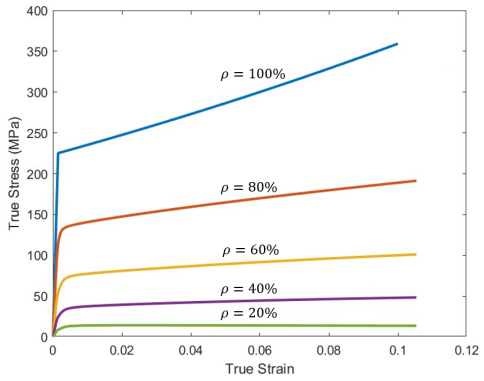

Fig. 4 True stress-strain curves of simulated compression specimens of different relative densities for model 2 boundary conditions.

Similar curves were obtained for the other boundary models (models 1, 3, 4). The elastic modulus, the yield stress and the tangent modulus of each case were obtained. These results are summarized in Table 1.

The main observations are that the principal differences between the models are found in the plastic zone. Indeed, the tangent modulus presents the largest deviations for different boundary conditions, especially for the low densities. Contrarily, the elastic modulus and the yield stress do not show important variations for the different models (5% or less). In general, the model with the lowest mechanical properties is model 1, which was expected since this model represents a single cell, so its bars are more prone to bending or buckling. This model, representative of a single cell has poor real applications, its interest is to provide a lower limit of the mechanical properties in lattice structures. Model 2 better simulates mechanical properties of lattice structures due to its 8-cell arrangement. However, it prevents by symmetry conditions some buckling that can happen in model 4. This latter model represents an array of 64 cells, and its lateral vertical bars can experience high deformations due to buckling. Model 3, the most constraint, is the stiffest, having the highest mechanical properties. This model represents an 8-cell lattice structure but in the ideal case in which its lateral faces will always remain flat, in spite of the values of the displacements. Model 3 aims to simulate a lattice structure portion that is inside a larger array, gaining resistance from contact with the surrounding cells or bulk material. Despite being an ideal case whose application in experiments is unlikely, it serves to establish an upper limit in terms of mechanical properties of lattice structures subjected to compression. It is expected that when simulating lattice structures with a larger number of cells, but with the boundary conditions of models 2 or 4, their behavior will tend to approach that of model 3 as the number of cells in the structure increases and the bending or buckling of the vertical external edge face becomes less relevant for the whole structure. This difference in mechanical properties due to changes in boundary conditions is exacerbated in structures with lower relative density, since they imply smaller diameter in the struts. This slenderness tends to increase the buckling in these struts, resulting in lower mechanical properties and even a softening effect once the plastic zone is reached. These effects are shown in Fig. 5, which shows the true stress-strain curves for the lattice structure at 20% and 40% of density fraction for the different boundary condition cases analyzed.

Table 1 Mechanical properties of simulated lattice structures at different relative densities and different boundary conditions. The maximum absolute difference (Δ) between the results for each relative density is computed, its percentage relative to the smallest result of the simulations of this case is also provided.

Relative density	Boundary condition	Elastic modulus (GPa)		Yield stress (MPa)		Tangent modulus (GPa)	
20%	Model 1	6.433	Δ= 0.113	12.6	Δ= 0.4	-0.026	Δ= 0.057
	Model 2	6.487	= 1.76%	12.8	= 3.17%	-0.008	= 219.23%
	Model 3	6.546		13.0		0.031	
	Model 4	6.526		13.0		0.010	
40%	Model 1	18.562	Δ= 0.243	33.2	Δ= 1.5	0.078	Δ= 0.033
	Model 2	18.675	= 1.31%	33.9	= 4,52%	0.103	= 42.31%
	Model 3	18.789		34.7		0.111	
	Model 4	18.805		34.5		0.109	
60%	Model 1	41.706	Δ= 0.659	69.6	Δ= 4.2	0.227	Δ= 0.012
	Model 2	42.015	= 1.58%	71.7	= 6.03%	0.233	= 5.29%
	Model 3	42.309		73.8		0.239	
	Model 4	42.365		73.3		0.239	
80%	Model 1	85.604	Δ= 1.063	132.6	Δ= 1.6	0.504	Δ= 0.012
	Model 2	86.065	= 1.24%	133.9	= 1.21%	0.509	= 2.38%
	Model 3	86.553		135.1		0.516	
	Model 4	86.667		134.2		0.516	
100% (Bulk material)		14.940		226.7		0.927	

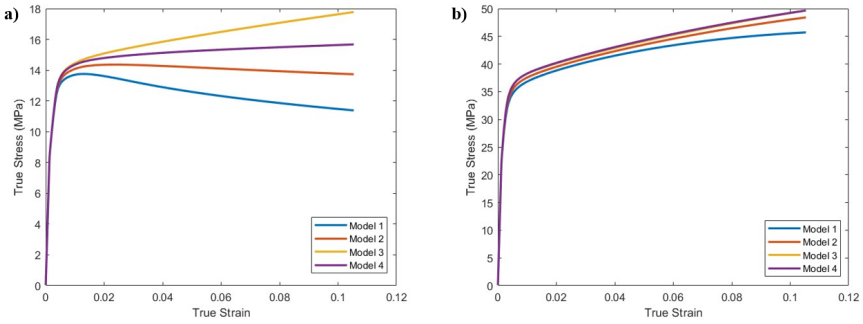

Fig. 5 True stress-strain curves of simulated compression specimens at (a) 20% and (b) 40% for different boundary condition models.

As it can be observed Fig. 5a, in the extreme case of structures with low densities (20%), a large difference in the mechanical properties is observed, especially in the tangent modulus, presenting a softening effect in the plastic zone for models 1 and 2 due to the buckling in the vertical bars at the edge of the structure. This behavior implies that to have a better mechanical response, an arrangement with a larger amount of cells should be considered. In Fig. 5, the results of model 4 (64 cells) and particularly of model 3 present ideal cases without buckling. These findings show the importance of the size effect on lattice structure, especially in the ones with low densities or small strut diameters. For the 40% relative density structure, no softening is observed, but there is still a considerable difference in the tangent modulus between the different models (up to 30%). Figure 6 shows the predicted deformed cells of model 1 at different densities, in which the buckling effect of the exterior vertical struts can be observed.

A Gibson-Ashby fit was performed for each model, varying the relative density. The adjustment curves are shown in Fig. 7, where it is observed that the Gibson-Ashby power function with C=1 predicts with good precision the three relative mechanical properties as a function of the relative density. The Gibson-Ashby curves for the Young modulus and yield stress almost overlap each other, reaffirming that these properties do not present significant changes when the number of cells in the structure (expressed as the boundary condition model) changes. The only boundary model

impact is observed in the tangent modulus, where a variation in the number of cells of the structure leads to an important change in this property and therefore in the associated curve.

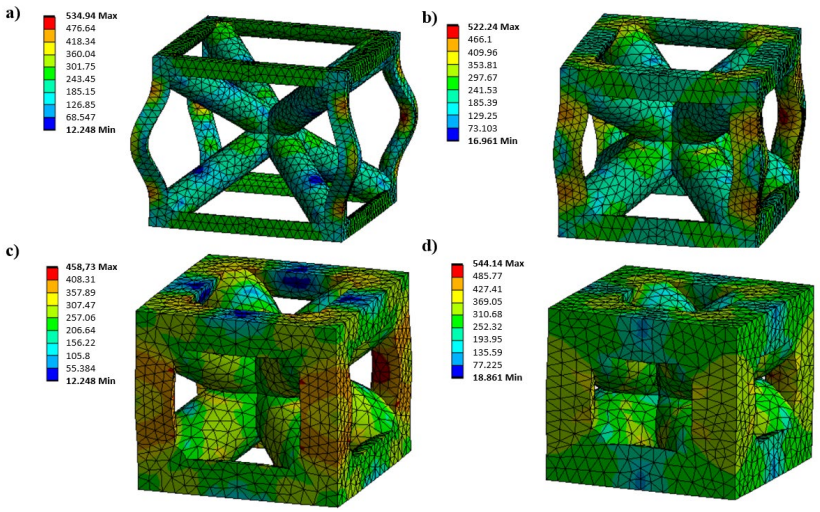

Fig. 6 Deformed simulated lattice structure with maps of von Mises equivalent stress for model 1 boundary conditions at (a) 20%, (b) 40%, (c) 60% and (d) 80% relative density for a macro strain of 10%.

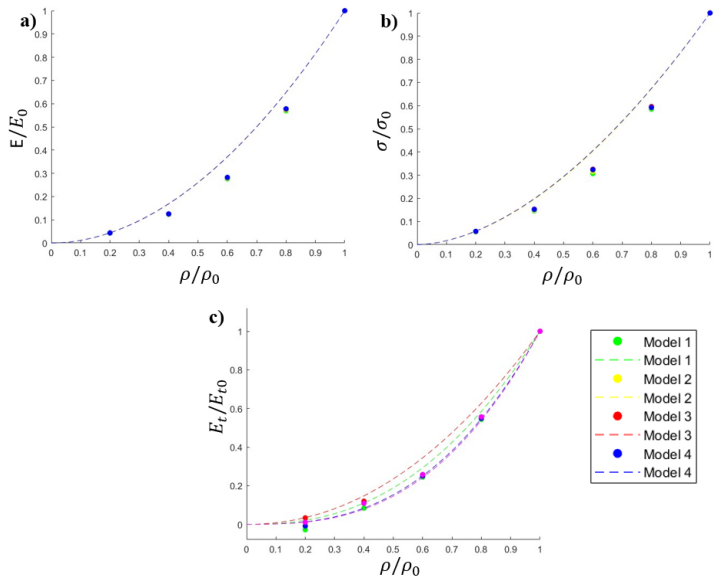

Fig. 7 Gibson-Ashby curves for different boundary condition models relating (a) relative elastic modulus, (b) yield stress and (c) tangent modulus. Symbols correspond to simulation results, dashed lines are the fitted Gibson-Ashby curves.

Conclusions

During this research, numerical simulations of body-centered cubic lattice cells with several densities and different boundary conditions were performed to determine the elastoplastic edge effect response. From the analysis of the results, the following main statements are derived:

- Size effect, represented by different boundary conditions, significantly affects the plastic response of the lattice structure. This effect is most remarkable for the tangent modulus, particularly in structures with low relative density and therefore small strut diameter. Their slenderness tends to cause strut buckling. Size effect induces reduced mechanical

properties in structures with a low number of cells, where this buckling tends to play a relevant role in the general behavior of the structure.

- The Gibson-Ashby model predicts both the elastic modulus and the yield stress with good precision and low size effect. To predict the plastic zone properties, such as the tangent modulus, size effect must be taken into account, since considerable change in the exponent of the Gibson-Ashby formula is observed for the different boundary condition models.

Ongoing research will focus on correlating these numerical results with experiments to validate the adopted methodology. In addition, for impact and energy absorption applications, the evaluation of the behavior of structures with different numbers of cells and at stages of larger deformation or densification should be considered.

Acknowledgements
This work is funded by WBI/AGCID RI02 (DIE23-0001) bilateral project between the University of Liège and the Universidad de La Frontera. As research director of F.R.S.-FNRS, A.M. Habraken thanks the Fund for Scientific Research for financial support.

References

[1] Valle R, Pincheira G, Tuninetti V, et al (2022) Evaluation of the Orthotropic Behavior in an Auxetic Structure Based on a Novel Design Parameter of a Square Cell with Re-Entrant Struts. Polymers (Basel) 14:4325. https://doi.org/10.3390/polym14204325

[2] Rilling S, Ríos I, Gómez Á, et al (2023) Optimized infill density through topological optimization increases strength of additively manufactured porous polylactic acid. Int J Adv Manuf Technol. https://doi.org/10.1007/s00170-023-12554-z

[3] Almesmari A, Alagha AN, Naji MM, et al (2023) Recent Advancements in Design Optimization of Lattice-Structured Materials. Adv Eng Mater 25:. https://doi.org/10.1002/adem.202201780

[4] Valle R, Pincheira G, Tuninetti V, et al (2022) Design and Characterization of Asymmetric Cell Structure of Auxetic Material for Predictable Directional Mechanical Response. Materials (Basel) 15:. https://doi.org/10.3390/ma15051841

[5] Maconachie T, Leary M, Lozanovski B, et al (2019) SLM lattice structures : Properties , performance , applications and challenges. Mater Des 183:108137. https://doi.org/10.1016/j.matdes.2019.108137

[6] Favre J, Lohmuller P, Piotrowski B, et al (2018) A continuous crystallographic approach to generate cubic lattices and its effect on relative stiffness of architectured materials. Addit Manuf 21:359–368. https://doi.org/10.1016/j.addma.2018.02.020

[7] Wang C, Zhu J, Wu M, et al (2021) Multi-scale design and optimization for solid-lattice hybrid structures and their application to aerospace vehicle components. Chinese J Aeronaut 34:386–398. https://doi.org/10.1016/j.cja.2020.08.015

[8] Syrlybayev D, Perveen A, Talamona D (2023) Experimental investigation of mechanical properties and energy absorption capabilities of hybrid lattice structures manufactured using fused filament fabrication. Int J Adv Manuf Technol 125:2833–2850. https://doi.org/10.1007/s00170-023-10922-3

[9] Zhang K, Shi D, Wang W, Wang Q (2017) Mechanical characterization of hybrid lattice-to-steel joint with pyramidal CFRP truss for marine application. Compos Struct 160:1198–1204. https://doi.org/10.1016/j.compstruct.2016.11.005

[10] Pasini C, Pandini S, Ramorino G, Sartore L (2024) Journal of the Mechanical Behavior of Biomedical Materials Tailoring the properties of composite scaffolds with a 3D-Printed lattice core and a bioactive hydrogel shell for tissue engineering. J Mech Behav Biomed Mater 150:106305. https://doi.org/10.1016/j.jmbbm.2023.106305

[11] Xu F, Zhang X, Zhang H (2018) A review on functionally graded structures and materials for energy absorption. Eng Struct 171:309–325. https://doi.org/10.1016/j.engstruct.2018.05.094

[12] Pirinu A, Primo T, Del Prete A, et al (2023) Mechanical behaviour of AlSi10Mg lattice structures manufactured by the Selective Laser Melting (SLM). Int J Adv Manuf Technol 124:1651–1680. https://doi.org/10.1007/s00170-022-10390-1

[13] Wang Z, Zhou Y, Wang X, Wei K (2021) International Journal of Mechanical Sciences Compression behavior of strut-reinforced hierarchical lattice — Experiment and simulation. Int J Mech Sci 210:106749

[14] Ashby MF (2006) The properties of foams and lattices. Philos Trans R Soc A Math Phys Eng Sci 364:15–30. https://doi.org/10.1098/rsta.2005.1678

[15] Rodrigo C, Xu S, Durandet Y, et al (2023) Quasi-static and dynamic compression of additively manufactured functionally graded lattices: Experiments and simulations. Eng Struct 284:115909. https://doi.org/10.1016/j.engstruct.2023.115909

[16] Gibson LJ AM (1997) Cellular Solids: Structure and Properties, 2nd ed

[17] Zadpoor AA (2019) Mechanical performance of additively manufactured meta-biomaterials. Acta Biomater 85:41–59. https://doi.org/10.1016/j.actbio.2018.12.038

[18] Bruson D, Galati M, Calignano F, Iuliano L (2023) Mechanical Characterisation and Simulation of the Tensile Behaviour of Polymeric Additively Manufactured Lattice Structures. Exp Mech. https://doi.org/10.1007/s11340-023-00976-5

[19] Köhnen P, Haase C, Bültmann J, et al (2018) Mechanical properties and deformation behavior of additively manufactured lattice structures of stainless steel. Mater Des 145:205–217. https://doi.org/10.1016/j.matdes.2018.02.062

[20] Maskery I, Aboulkhair NT, Aremu AO, et al (2017) Compressive failure modes and energy absorption in additively manufactured double gyroid lattices. Addit Manuf 16:24–29. https://doi.org/10.1016/j.addma.2017.04.003